EFFECT OF FIBER DISPERSION ON MULTIPLE CRACKING OF CEMENT COMPOSITES

By Yilmaz Akkaya,[1] Surendra P. Shah,[2] and Bruce Ankenman[3]

ABSTRACT: High performance, fiber-reinforced composites are identified by their high strength and toughness associated with multiple cracking. If the composite is adequately reinforced, the bridging fibers will transfer the load and multiple cracking will occur when the subsequent transferred load cracks the matrix again. This study investigates the effect of dispersion of fibers on the multiple cracking behavior of fiber-reinforced composites. The electronic speckle pattern interferometry technique is used to record the location of crack initiation, the sequence of the multiple cracking, and the corresponding cracking stresses. Microstructural parameters at each crack location are statistically quantified by the theory of point processes. The size of the fiber-free areas and the fiber clumping are calculated at the crack cross sections. By using linear elastic fracture mechanics, the fracture toughness of the matrix is calculated. A strong relation between the cracking stress and the fiber-free areas in the composite is observed. It is shown that the toughness of the composite depends on the fiber clumping at the first crack cross section.

INTRODUCTION

High performance, fiber-reinforced composites are characterized by higher elastic limit, strain hardening, and toughness associated with multiple cracking. As the load increases on the composite, a flaw in the matrix may spread over the specimen cross section. The mechanics of this spread depends on the size of the flaw, the properties of the fiber reinforcement, and the matrix toughness. If the composite is adequately reinforced, the bridging fibers will share the load and transfer it to the other parts of the composite. Multiple cracking occurs when the subsequent transferred load cracks the matrix again. Hence, the initial flaw size and the fiber dispersion play an important role in the initiation of the cracking and the toughness (Shah and Ouyang 1991; Li and Wu 1992; Betterman et al. 1995; Li and Maalej 1996; Shao and Shah 1997).

Akkaya et al. (2000a) reported that, under certain circumstances, better dispersion of shorter fibers improves mechanical properties of the composites as compared with longer fibers. Experimental results with fiber-reinforced extruded cement composites, made with an identical fiber volume fraction of 3%, indicated that composites with 2 mm long fibers failed with an enhanced postpeak behavior with multiple cracks, whereas composites with 6 mm long fibers did not exhibit multiple cracking. Microstructural studies confirmed that the shorter fibers disperse better than the longer fibers, and this in in turn increased the toughness performance of the composites.

This study investigates the effect of fiber dispersion on the sequential multiple cracking of extruded fiber-reinforced composites. Extrusion is a forming process, which forces highly viscous, dough-like plastic mixture through a rigid opening (a die) having a desired cross-sectional geometry. Materials form under high shear and compressive forces, which can lead to improved interfacial bond and aligned fibers (Shao et al. 1997; Akkaya et al. 2000a,c). The electronic speckle pattern interferometry (ESPI) technique is used to observe the multiple cracking of the material and to evaluate the cracking stresses of the composite. The ESPI technique is a highly accurate displacement measurement method, which allows mapping of the crack propagation at the microscale.

Microstructural parameters at each crack location are quantified, and the size of the fiber-free areas and percentage of the fiber clumping in the composite are calculated by point process statistics. Each fiber is realized as a point in the analysis, and the relationship among fiber distances is investigated. A strong relation between the cracking stress and the size of the fiber-free areas in the composites is observed. By using this relation, fracture toughness of the matrix is calculated by linear elastic fracture mechanics (LEFM). It is also shown that the toughness of the composite depends on the fiber clumping at the first crack cross section of the composite.

MATERIALS AND EXPERIMENTAL TECHNIQUES

PVA fibers of 14 microns in diameter and 2 mm in length are used in the experiments. The elasticity modulus and the tensile strength of the fibers were 41 GPa and 1,900 MPa, respectively. The basic mix design of the composite was (by volume) 45% cement, 12% silica fume, 3% fibers, 1% superplasticizer, and 39% water, with a 0.29 water/cement ratio (by weight).

Mixing procedure was as follows: First, fibers and liquids are mixed together for two minutes, then the solids are added and all the components are mixed for another 10 minutes. Specimens are produced by extrusion of the fresh composite. A ram type extruder mounted on a material testing system machine is used to process the specimens under stroke control. A die with a rectangular cross section of 25.4×4 mm is used during extrusion. Details of the extruder can be found in Shrinavasan et al. (1999). After 24 hours from extrusion, specimens are placed in steam curing at 90°C for two days. Thereafter, they are kept in a constant temperature and humidity of 20°C and 50 RH% for three days. Then the specimens are oven-dried at 105°C for 24 hours and tested in flexure after another 24 hours.

Flexural behavior of the composites is studied to evaluate the mechanical performance. A closed-loop, four-point flexure test is performed by controlling the displacement measured by a linear variable differential transducer (LVDT) mounted on the specimen (Fig. 1). Specimens are loaded at a rate of 3×10^{-5} mm/s. The gauge length was 38.1 mm. The resulting load versus displacement data is recorded. Five identical specimens are tested. Flexure tests are followed with the ESPI technique to record the location of crack initiation and the sequence of the multiple cracking.

The electronic speckle pattern interferometry (ESPI) tech-

[1]Grad. Student, Northwestern Univ., School of Engrg. and Appl. Sci., Evanston, IL 60208.

[2]Walter P. Murphy Prof., Dir. of ACBM, Northwestern Univ., School of Engrg. and Appl. Sci., Evanston, IL 60208.

[3]Asst. Prof., Northwestern Univ., School of Engrg. and Appl. Sci., Evanston, IL 60208.

Note. Associate Editor: Farhad Ansari. Discussion open until September 1, 2001. To extend the closing date one month, a written request must be filed with the ASCE Manager of Journals. The manuscript for this paper was submitted for review and possible publication on May 24, 2000; revised November 7, 2000. This paper is part of the ***Journal of Engineering Mechanics***, Vol. 127, No. 4, April, 2001. ©ASCE, ISSN 0733-9399/01/0004-0311–0316/$8.00 + $.50 per page. Paper No. 22337.

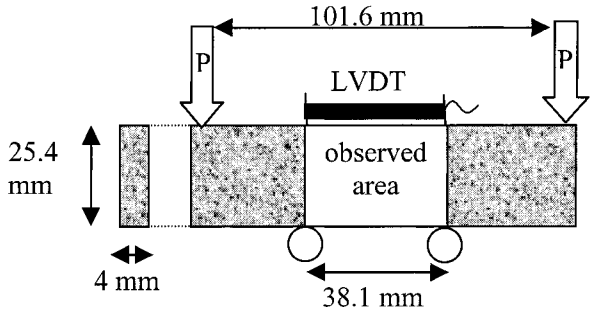

FIG. 1. Dimensions of Test Specimen

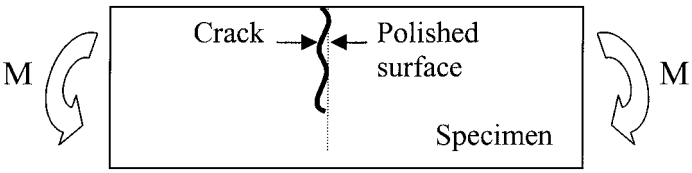

FIG. 2. Polished Crack Cross Section of Composite

nique is a highly accurate displacement measurement method, which allows mapping of the crack propagation at the microscale. The experimental setup includes an interferometer, a loading unit, image acquisition and processing units, an analog/digital interface, and an image storage and display. A 45 mW helium-neon laser is used as the light source. The test is followed by a CCD camera to record the speckle patterns. The scattered images of the reference and the deformed states of the composite and load-displacement values are recorded. The speckle pattern fringes are formed by the electronic subtraction of the reference image and deformed image. Details about the technique and fringe formation can be found in Ghandehari et al. (1999).

Microstructural observations at the cross sections of crack locations are made by a scanning electron microscope (SEM), in order to understand the mechanisms involved in the composite failure. The specimens are cut at the fracture plane along the specimen width (Fig. 2). Polished specimens are prepared in order to study fiber dispersion and fiber-free areas in the composite. Statistical analysis is employed to quantify the fiber dispersion on the polished cross section. The relation between the microstructural parameters and the composite cracking is evaluated.

FIBER DISPERSION ANALYSIS

Fiber dispersion and the size and number of fiber-free areas play an important role in the initiation and sequence of the composite cracking. As the fibers clump and the size and number of matrix areas that are not supported by fibers increase, the initiation of a crack requires less energy, and once the crack forms, it can advance easily through the fiber-free areas in the matrix.

Point process statistics are calculated in order to quantify the dispersion of fibers (Diggle 1983; Akkaya et al. 2000b). SEM pictures of the polished crack surfaces are digitized; each fiber is marked and taken as a point in the image analysis program. Then the coordinates of each fiber are used to calculate the distances between fiber pairs. These distances are used to calculate the statistical point process functions. An area of 10 mm^2 on the cross-sectional surface, where the cracking initiated is used for analysis. Further information about specimen preparation can be found in Akkaya et al. (2000a).

Two statistical functions are calculated to quantitatively describe the fiber dispersion. The K-function is a standard measure of the expected number of fibers within a certain distance of a given fiber location [Fig. 3(a)]. The K-function is calculated to describe the tendency of fibers to clump. The F-function is the distribution of distances between arbitrary points to the nearest fiber, which can be used to describe the size of the fiber-free areas [Fig. 3(b)]. The F-function gives the probability of any point in the cross section being at least a distance r away from the nearest fiber.

The K-function is the normalized number of fibers within a distance r of a given fiber. For the estimator of the K-function, the following formula is used:

$$K(r) = \frac{\text{number of fibers within } r \text{ of a given fiber}}{(\text{total number of fibers in the observation area})^2} \cdot (\text{Area of the observed region}) \quad (1)$$

where r = distance from the fiber. In order to analyze if the fiber dispersion of the composites is perfectly random or if

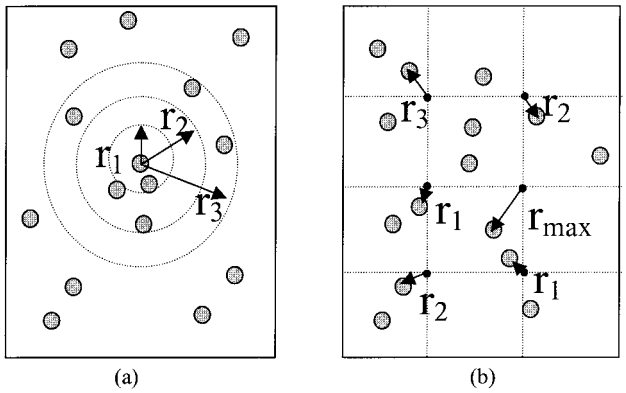

FIG. 3. Calculation of: (a) K-Function; (b) F-Function

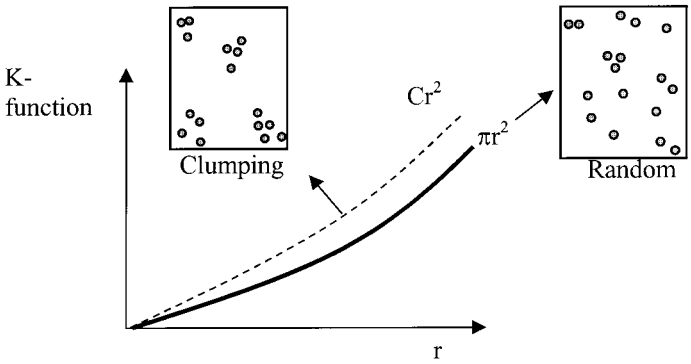

FIG. 4. Comparison of Clumping and Random Dispersion

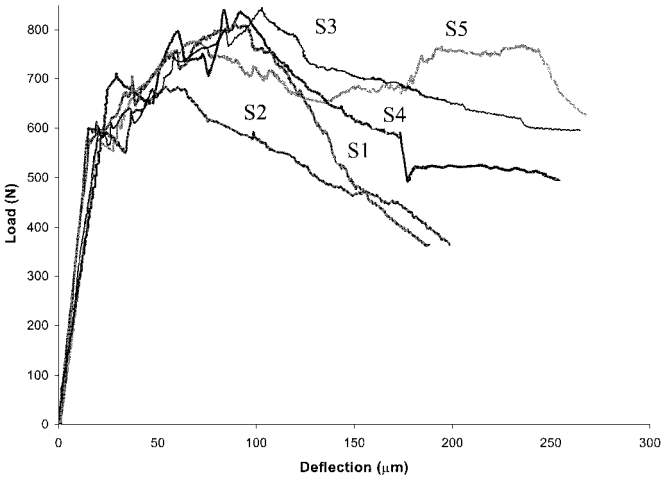

FIG. 5. Four-Point Flexure Test Results of Identical Composites

J. Eng. Mech. 2001.127:311-316.

they show any clumping behavior, reference random data points (Poisson distribution) are used. This random dispersion is compared with the fiber dispersion of the crack locations. For a complete spatial random dispersion, the K-function would be πr^2 (Fig. 4). K-functions on the upper side of random dispersion would indicate clumping, since the number of fibers at a certain distance from a given fiber is increasing. K-functions on the lower side of random dispersion would indicate a regular dispersion. Percentage of clumping in the composite with respect to the random dispersion can be calculated by

$$\% \text{ Clumping} = \left(\frac{C}{3.14} - 1\right) \times 100 \tag{2}$$

where C = constant term in Cr^2, the curve fit to the K-function of the fiber dispersion at the crack cross section.

Estimation of the F-function is achieved by laying down a regular grid of points on the observed region (4,961 points were used), and then finding the nearest fiber to each grid point. The largest of these arbitrary point-nearest fiber distances is the radius of the maximum fiber-free area [Fig. 3(a)]. The following estimator is used for the F-function:

TABLE 1. Cracking Stresses, Maximum Stresses, and Corresponding Displacements of Composites

Specimen number (1)	Crack number (2)	Cracking stress (MPa) (3)	Maximum fiber-free area size (μm) (4)	Displacement at first crack (μm) (5)	Maximum stress (MPa) (6)	Displacement at maximum stress (μm) (7)	Toughness ratio (%) (8)	Clumping at first crack (%) (9)
S1	1	25.5	381	16.3	36.0	88.6	5.4	47
	2	28.1	271					
	3	29.3	226					
	4	29.3	223					
	5	29.7	219					
	6	31.1	209					
S2	1	26.2	393	15.5	30.2	54.0	3.5	56
	2	27.1	316					
	3	28.0	284					
	4	29.2	232					
S3	1	26.8	400	20.7	37.4	102.7	5.0	48
	2	28.2	310					
	3	35.3	219					
S4	1	30.2	342	26.0	37.2	83.4	3.2	60
	2	33.1	284					
S5	1	25.6	335	20.4	34.5	193.0	9.5	11
	2	32.8	209					

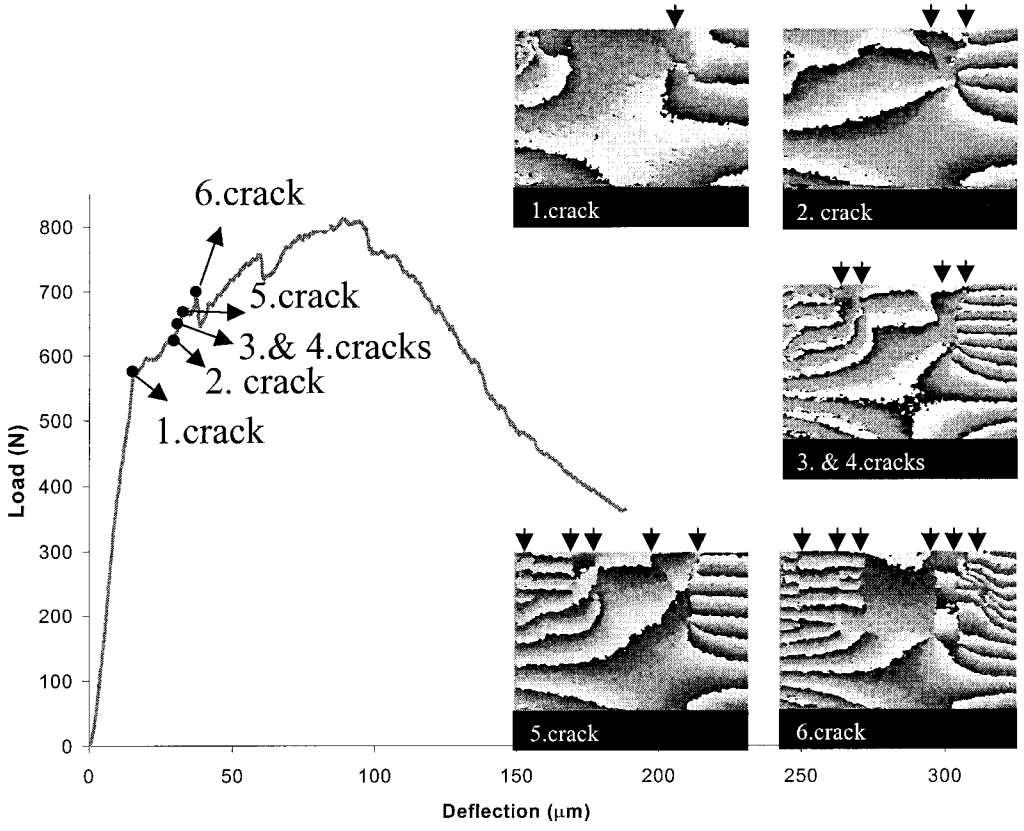

FIG. 6. ESPI Pictures of Specimen, Taken during Test, and Locations and Sequence of Cracks

J. Eng. Mech. 2001.127:311-316.

$$F(r) = \frac{\text{number of grid points whose nearest fiber is less than } r \text{ away}}{\text{total number of grid points}} \tag{3}$$

Since the compliment of this function would indicate the fraction of the total fiber-free area, $1 - F(r)$ is calculated. High values of $1 - F(r)$ indicate the increase in the fiber-free areas. If the fibers exhibited complete spatial randomness, then the F-function would take the form $1 - \exp(-\pi\lambda r^2)$, where λ = number of fibers in the observation area.

LINEAR ELASTIC FRACTURE MECHANICS

Fiber-reinforced cement composites contain preexisting flaws and defects. It is the size of these flaws that determines the critical load required for crack initiation. Far-field stresses, well away from the location of the flaw, will be equal to the applied stress σ_a. However, the presence of the flaw along the cross section perpendicular to the applied load would cause stress concentration at the tip of the flaw. Here, the flaw is considered to be in an infinite plane, traction-free and subjected to uniaxial tensile stress. According to the principles of linear elastic fracture mechanics (LEFM) (Irwin 1957), stresses at the flaw tip are proportional to a factor called the stress intensity factor, K_I, which can be derived by basic principles of elasticity. A general expression for K_I would be

$$K_I = \sigma_a \sqrt{\pi a} f\left(\frac{a}{b}\right) \tag{4}$$

where a = flaw size; and $f(a/b)$ accounts for the geometry of the structure. Various K_I solutions for different geometry can be found in fracture mechanics books (Tada et al. 1985; Anderson 1995; Shah et al. 1995). K_I increases proportionally with the applied load, and at a critical value, K_{IC}, failure occurs. LEFM is applicable as long as the initial flaw size can be considered unchanged. In this study, LEFM is used to calculate the fracture toughness at the crack initiation.

For an edge cracked plate subjected to pure bending, the K_I solution is given (Anderson 1995) as

$$f\left(\frac{a}{W}\right) = \frac{K_I B W^{3/2}}{M} = \frac{\sqrt{\frac{6}{\pi}\tan\left(\frac{\pi a}{2W}\right)}}{\cos\left(\frac{\pi a}{2W}\right)}\left[0.0923 + 0.199\left\{1 - \sin\left(\frac{\pi a}{2W}\right)\right\}^4\right] \tag{5}$$

where B = specimen thickness; W = specimen width; a = flaw size; and M = moment. Fracture toughness K_{IC} can be calculated by (5) using the moment and flaw size at which the opposite cracking occurs.

TEST RESULTS AND ANALYSIS

Fig. 5 gives the four-point bending test results of the identical composites. Cracking stresses, maximum stresses, and corresponding displacements are given in Table 1. ESPI pictures of cracks of one of the samples are presented in Fig. 6. This figure presents the crack initiation locations and corresponding stresses and displacements. For this composite, a total of six cracks have been observed and examined. Crack locations can be identified by discontinuities in the fringes of ESPI pictures. The number of cracks examined in the other specimens can be found in Table 1.

In order to prepare the test specimens for further analysis, each specimen is separated from the main crack location and polished, and an SEM picture of the cross section is taken. Then the specimen is polished until all the other crack cross sections are exposed and SEM pictures taken. Fig. 7(a) presents the SEM pictures of the crack surfaces of the same composite. Fig. 7(b) presents the pictures used in the image analysis program to obtain the coordinates of each fiber. Then the distances between fiber pairs and the point process statistics are calculated.

The result of the K-function is given in Fig. 8. Crack cross sections with evenly dispersed fibers can be identified by their closeness to the random dispersion. As it can be seen from the figure, first, second, and third crack cross sections have higher K-function values, meaning a greater number of fibers can be found around a fiber. Cross sections with a higher degree of fiber clumping would crack before cross sections with evenly dispersed fibers. Fourth, fifth, and sixth cracks exhibited fiber dispersions similar to the random dispersion. Fig. 9(a) presents the result of the (1-F)-function. At the first crack location, as

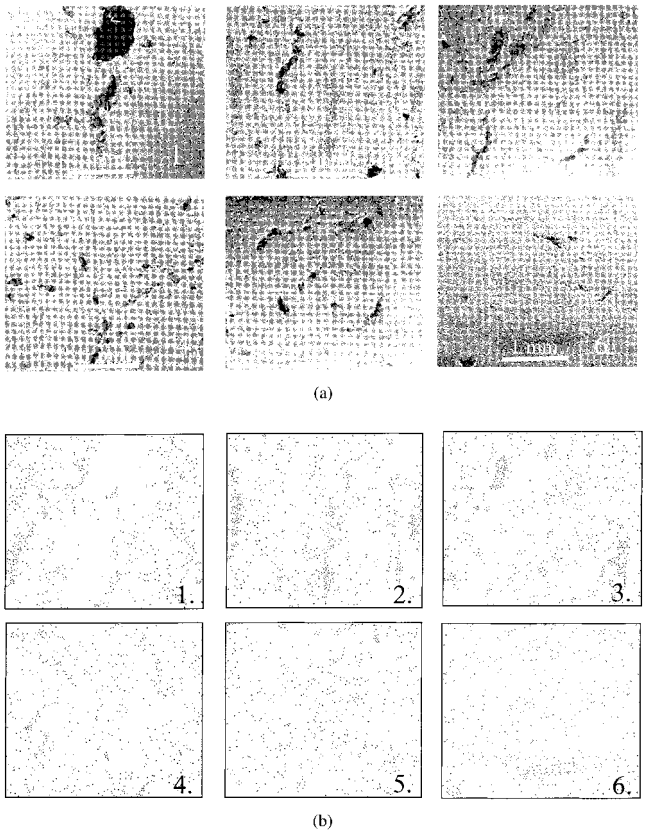

FIG. 7. (a) SEM Pictures of Sequential Crack Locations (×50); (b) Pictures Used in Image Analysis Program

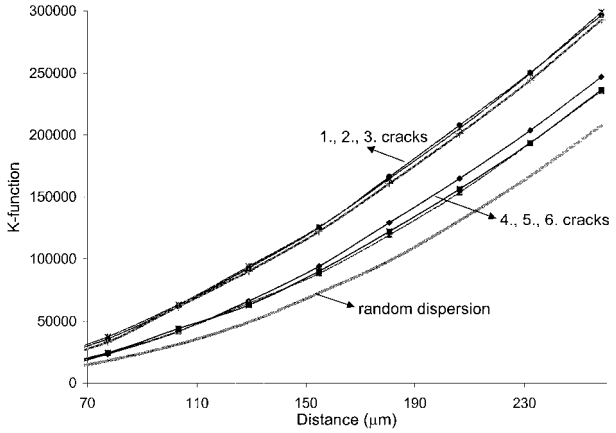

FIG. 8. K-Function of Fiber Dispersions at Crack Cross Sections and Random Dispersion

J. Eng. Mech. 2001.127:311-316.

it can be seen from the figure, the number of fiber-free areas observed are more than the subsequent cracks. These fiber-free areas act as defects in the composite and decrease the mechanical performance. Fig. 9(b) presents the comparison of the largest fiber-free area size. The largest fiber-free area is found at the first crack location. The size of the largest fiber-free areas found at the crack locations of all specimens can be found in Table 1.

K_{IC} values of the matrices are calculated by (5). Experimental values of cracking loads are used to calculate the moments, and the radius of the largest fiber-free area is used as the flaw size. K_{IC} values are calculated for each crack of the specimen and their averages are used to calculate the K_{IC} value of the paste. For five specimens, K_{IC} values are calculated as 24, 24, 25, 27, and 29 MPa $mm^{1/2}$ (Fig. 10). A 95% confidence interval for the average K_{IC} value for the paste is then (23.1, 28.5) MPa $mm^{1/2}$. The interval contains the value 26 MPa $mm^{1/2}$, reported by Ouyang et al. (1992) for a cement paste with a similar mix design. A K_{IC} value of 20 MPa $mm^{1/2}$ is reported by Mobasher et al. (1991) and Jenq et al. (1986) for a cement paste with a higher water to cement ratio.

Akkaya et al. (2000a) also used extruded composites, with the same mix design, in three-point bending tests with a different specimen geometry (thickness: 25 mm; width: 4 mm; span: 101.6 mm). Since the span to width ratio of the specimens is too large, K_{IC} formulation of the pure bending [(5)] is used. The limit of proportionality of the load-deformation curves is used as the first cracking loads of the specimens. Average size of the fiber-free areas (a = 370 microns), calculated from the four-point bending specimens, is used as the defect size at the first crack. K_{IC} values of 23, 24, 24, 24, 26, and 27 are calculated from six samples. The 95% confidence interval for the average K_{IC} of the paste from this data is (23.1, 26.3). Again the interval contains the K_{IC} = 26 MPa $mm^{1/2}$ value reported by Ouyang et al. (1992).

Fig. 11 presents the cracking load versus defect size values. Eq. (5) is also plotted in the figure with K_{IC} = 26 MPa $mm^{1/2}$. In both the theoretical model and the data, load increases as the size of the fiber-free areas decreases. In the above calculations, it is assumed that the largest fiber-free area is equal to the flaw size of the matrix. In reality, the initial flaw size of this rather dense cement paste matrix is likely to be smaller than the largest fiber-free area. However, if one assumes that, once the flaw initiates it will propagate with a constant K_{IC} until arrested by the fiber, then the calculation of K_{IC} performed here may be acceptable. It should also be noted that in this simplifying calculation, any possible interaction between cracks is not accounted for.

Toughness of the composite is expressed by the ratio of displacement at the maximum stress to the displacement at the first cracking stress, evaluated from the four-point flexure test (Table 1). A variation in toughness can be seen among the identical specimens. Microstructural parameters are used to explain the different behavior among the samples. The percentage of fiber clumping at the crack locations is calculated by (2) (Table 1). A close relationship between the fiber dispersion at the first crack location and the composite toughness is seen

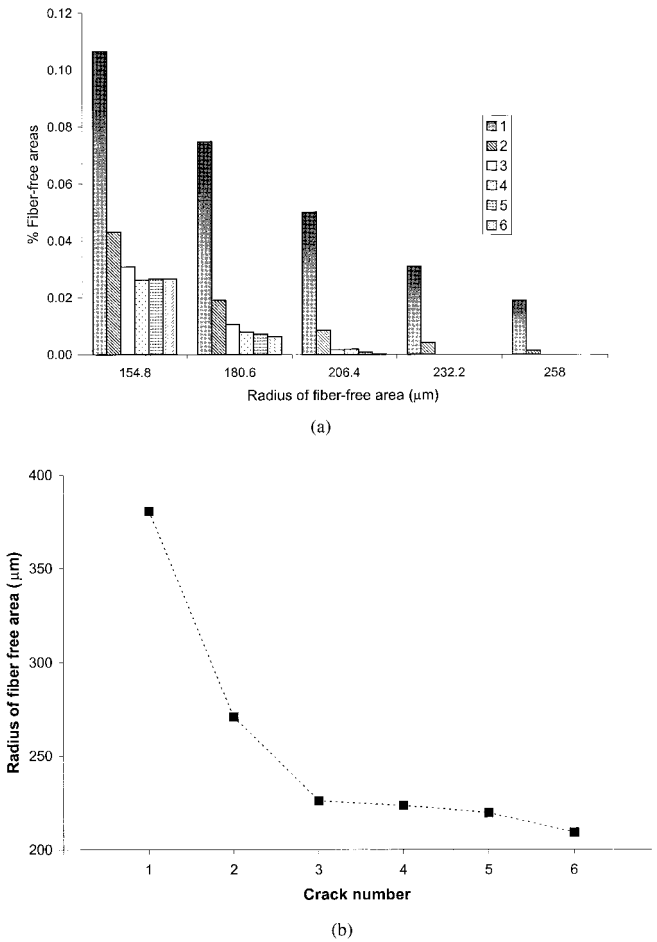

FIG. 9. (a) (1-F)-Function Values of Sequential Cracks; (b) Comparison of Largest Fiber-Free Area at Crack Locations

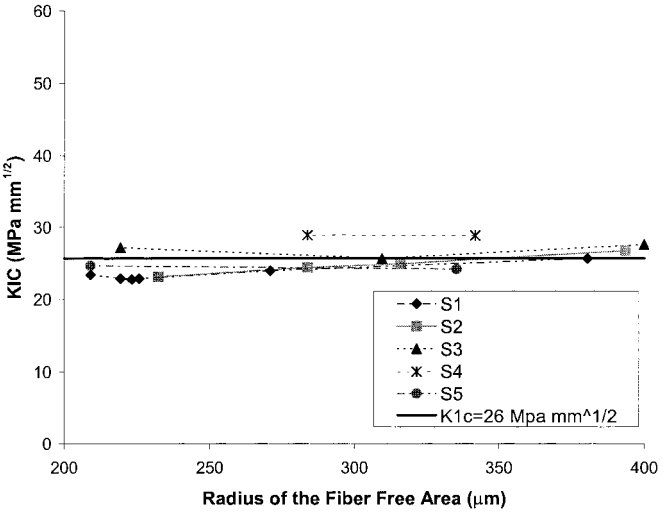

FIG. 10. K_{IC} versus Defect Size of Specimens

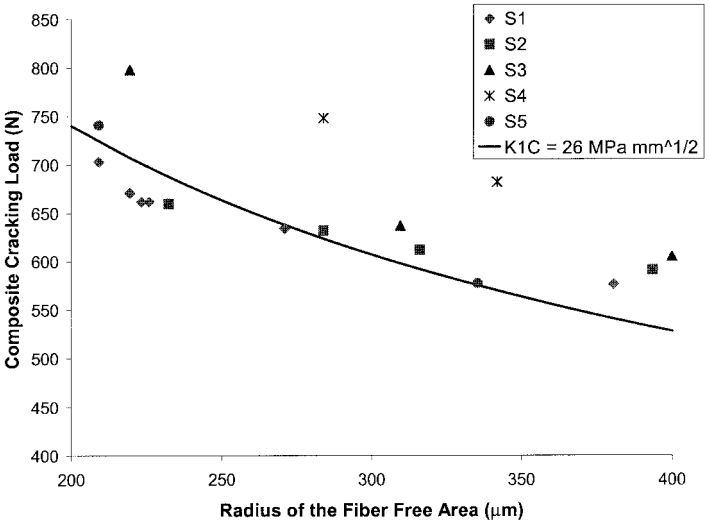

FIG. 11. Comparison of Theoretical and Experimental Cracking Stress versus Defect Size

J. Eng. Mech. 2001.127:311-316.

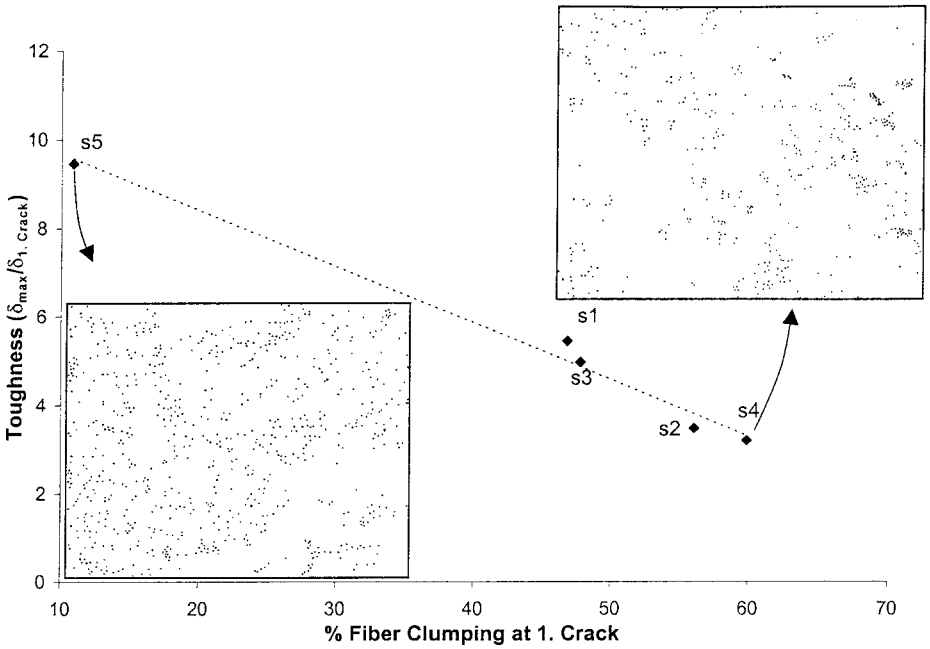

FIG. 12. Effect of Fiber Clumping at First Crack Location on Specimen Toughness

in Fig. 12. SEM pictures of fiber dispersion at first crack locations of the specimens with highest and lowest toughness values are also compared in the figure. An efficient fiber bridging and transfer of the load to other parts of the composite can be achieved if there is a better fiber dispersion and less fiber clumps at the first crack location. Better fiber dispersion, in turn, increases the toughness of the composite.

In previous research (Akkaya et al. 2000a), mechanical performance of fibers has been related to the bond characteristics and the pullout performance of the fibers. The results of this research indicate that the dispersion of fibers can also play a significant role in the first crack stress and multiple cracking response of the composites.

CONCLUSION

Microstructural parameters such as the size of the fiber-free areas and the fiber dispersion in the composite are associated with the mechanical performance and sequential multiple cracking of the fiber-reinforced cement-based composites. These parameters can be quantified by using the statistical approach described in this study. It is seen that fiber-free areas reduce the cracking stress of the composite by acting as defects in the material. Sequential cracks form depending on the size of the fiber-free areas at the composite cross section.

The K_{IC} of the extruded matrix is calculated as 26 MPa $mm^{1/2}$, in accordance with the values reported for cement paste in the literature. This indicates that the procedure used to measure the size of the fiber-free areas is reasonably accurate and the linear elastic fracture mechanics assumptions are a good approximation for this cracking process.

Fiber dispersion affects the toughness of the composites by its role in transferring the load to the other parts of the specimen. An effective crack bridging and increase in the toughness of the composite can be achieved if the fiber dispersion is better at the first crack location.

ACKNOWLEDGMENT

The writers would like to thank the Center for Advanced Cement-Based Materials and the National Institute of Statistical Sciences for the funding of this research.

APPENDIX. REFERENCES

Akkaya, Y., Peled, A., and Shah, S. P. (2000a). ''Parameters related to fiber length and processing in cementitious composites.'' *Mat. and Struct.*, Paris, 33, 515–524.

Akkaya, Y., Picka, J., and Shah, S. P. (2000b). ''Spatial distribution of aligned short fibers in cement composites.'' *J. Mat. in Civ. Engrg.*, ASCE, 12(3), 272–279.

Akkaya, Y., Peled, A., Picka, J., and Shah, S. P. (2000c). ''Effect of sand addition on properties of fiber reinforced cement composites.'' *ACI Mat. J.*, 97(3), 393–400.

Anderson, T. L. (1995). *Fracture mechanics*, 2nd Ed., CRC Press, Boca Raton, Fla.

Betterman, L. R., Ouyang, C., and Shah, S. P. (1995). ''Fiber-matrix interface in microfiber-reinforced mortar.'' *Advances in Cement Based Mat.*, 1(2), 53–61.

Diggle, P. J. (1983). *Statistical analysis of spatial point patterns*, Academic, San Diego.

Ghandehari, M., Krishnaswamy, S., and Shah, S. (1999). ''Technique for evaluating kinematics between rebar and concrete.'' *J. Engrg. Mech.*, ASCE, 125(2), 234–241.

Irwin, G. R. (1957). ''Analysis of stresses and strains near the end of a crack traversing a plate.'' *J. Appl. Mech.*, 24, 361–364.

Jenq, Y., and Shah, S. P. (1985). ''Two parameter fracture model for concrete.'' *J. Engrg. Mech.*, ASCE, 111(10), 1227–1241.

Li, V. C., and Wu, H.-C. (1992). ''Conditions for pseudo strain-hardening in fiber reinforced brittle matrix composites.'' *Appl. Mech. Rev.*, 45(8), 390–398.

Li, V. C., and Maalej, M. (1996). ''Toughening in cement based composites. Part II.'' *Cement and Concrete Compos.*, 18, 239–249.

Mobasher, B., Ouyang, C., Castro-Montero, A., and Shah, S. P. (1991). ''Tensile behavior of fiber reinforced concrete.'' *Fracture process in concrete, rock and ceramics*, RILEM, Paris, 269–284.

Ouyang, C., and Shah, S. P. (1992). ''Toughening of high strength cementitious matrix reinforced by discontinuous short fibers.'' *Cement and Concrete Res.*, 22, 1201–1215.

Shah, S. P., and Ouyang, C. (1991). ''Mechanical behavior of fiber-reinforced cement-based composites.'' *J. Am. Ceramics Soc.*, 74(11), 2727–2738, 2947–2953.

Shah, S. P., Swartz, S. E., and Ouyang, C. (1995). *Fracture mechanics of concrete*, Wiley, New York.

Shao, Y., and Shah, S. P. (1997). ''Mechanical properties of PVA fiber reinforced cement composites fabricated by extrusion processes.'' *ACI Mat. J.*, 94(6), 555–564.

Shrinavasan, R., DeFord, D., and Shah, S. P. (1999). ''The use of extrusion rheometry in the development of extruded fiber reinforced cement composites.'' *Concrete Sci. and Engrg.*, 1(1), 26–36.

Tada, H., Paris, P. C., and Irwin, G. R. (1985). *The stress analysis of cracks handbook*, Paris Productions, St. Louis.

J. Eng. Mech. 2001.127:311-316.